J Mater Sci (2011) 46:5216–5220
DOI 10.1007/s10853-011-5458-z

Design, synthesis, and characterization of bulk metallic glass composite with enhanced plasticity

G. Y. Sun · G. Chen · G. L. Chen

Received: 28 November 2010 / Accepted: 9 March 2011 / Published online: 25 March 2011

Abstract A Zr-based bulk metallic glass (BMG) in situ composite with a designed composition of $Zr_{60}Ti_{14.67}Nb_{5.33}Cu_{5.56}Ni_{4.44}Be_{10}$ was prepared based on both modifying alloy composition and controlling solidification process. The composite contains high volume fraction of coarsen bcc β-Zr(Ti, Nb) solid solution. The β phase particles are short rod-like, worm-like, and nearly spherical in morphology rather than typical dendrite structure, their volume fraction and average diameter were estimated to be about 55% and 20 μm, respectively. The composite displays a large fracture strain up to 22.3% under uniaxial compression at room temperature. The coarse β phase and its high volume fraction were thought to be responsible for the excellent plastic deformability of the present composite.

Introduction

Bulk metallic glasses (BMGs) have very high yield strength approaching theoretical limit, but they lack plasticity and fail in an apparently brittle manner at ambient temperature and, therefore, usually are considered quasi-brittle materials [1–4]. During the past few years, enhancing plasticity of BMGs has attracted broad attention and considerable efforts have been devoted to the fabrication of BMG composites containing crystalline reinforcements in glassy matrix [5–11]. The presence of crystalline phase can prevent a single shear band from traversing through the sample and generate multiple shear bands [2]. Among the different BMGs developed so far, the most promising are the ductile metal-reinforced composites, in which the ductile inclusions precipitate during the cooling process by nucleation and dendritic growth [12, 13]. Further investigations demonstrated that the room-temperature mechanical properties of the BMG composites are very sensitive to the changes of the morphology, size, and volume fraction of the ductile phase. Especially, the size and volume fraction of the ductile phase is crucial for optimizing the ductility and fracture behavior [12].

In view of the above-mentioned facts, we developed an innovative method to produce Zr-based BMG in situ composites [14], which was based on controlling solidification in the liquid–solid two-phase region. The attempt is to coarsen the ductile inclusions dispersed in BMG matrix. As a result, a new kind of Zr-based BMG composite, labeled as composite S1, was prepared. Which consists of micro-sized spheres of bcc β-Zr(Ti, Nb) solid solution dispersed BMG matrix and exhibits substantially improvement in plasticity as compared with those with dendritic β phase inclusions [15]. Furthermore, another Zr-based BMG in situ composite, named as composite S2, was developed based on both controlling solidification and modifying composition. The underlying goal is to coarsen the ductile precipitates and simultaneously increase their volume fraction. Recently, Hofmann et al. reported Zr-based BMG

G. Y. Sun (✉)
School of Mechanical Engineering, North China University of Water Conservancy and Electric Power, Zhengzhou 450011, China
e-mail: gysun555@sohu.com

G. Chen · G. L. Chen
Joint Laboratory of Nanostructured Materials and Technology, Nanjing University of Science and Technology, Nanjing 210094, China

G. L. Chen
State Key Laboratory for Advanced Metals and Materials, University of Science and Technology Beijing, Beijing 100083, China

composites with high toughness and tensile ductility, which were developed by modifying alloy composition and treating alloy melt in their semi-solid two-phase region [3]. It seems that increasing the volume fraction of the ductile phase and, simultaneously coarsening these ductile inclusions, has become an effective approach to improve the plasticity of BMG composites.

As an evidence to support the validity of coarse ductile phases on improving the plasticity of the BMG composites, the compressive stress–strain curve for the composite S2 had been shown in [14]. Here, the alloy design principle and compositional modification method of the composite S2 will be presented. And then, the microstructure and room-temperature mechanical behavior are characterized in detail, the mechanism of the enhanced plasticity is revealed through observing the surface microstructures of the deformed compression samples.

Design of alloy composition

Previous studies on Zr–Ti–Nb–Cu–Ni–Al BMG composites [12] and Ti–Cu–Ni–Sn–Ta (Nb) nanostructured matrix materials (NsM) [16] showed that small changes in the composition of such complex alloys lead to strongly different solidification behavior because the alloys have more than five constituents between which intermetallics can easily form, which counteracts the reinforcement by the ductile β-phase dendrites and deteriorates the ductility of the composites. Therefore, compositional modification should be based on a detailed analysis of phase diagram so as to obtain a two-phase microstructure consisting only of ductile crystalline phase dispersed fully amorphous matrix.

Figure 1 shows a pseudo-ternary phase diagram with apexes of Zr, (Ti + Nb), and (Be_{50} + $Cu_{27.8}$ + $Ni_{22.2}$) [17]. The compositional points Vit.1 and C, H &S1 lie on the same line of $(Zr_{75}$ $(Ti_{25-x}Nb_x)$ $_{25})_{100-y}$ $(Cu + Ni + Be)_y$, they represent the compositions of $Zr_{41.2}Ti_{13.8}Cu_{12.5}Ni_{10}Be_{22.5}$ (Vit.1 alloy) and $Zr_{56.2}Ti_{13.8}Nb_{5.0}Cu_{6.9}Ni_{5.6}Be_{12.5}$, respectively. At the latter composition corresponding to the compositional point C, H &S1 in Fig. 1, Szuecs et al. fabricated two dendritic β-phase-containing BMG composites, labeled as C and H. The volume fraction of the β-phase was reported to be 25% for C and 20% for H. For the composite S1 with the same composition as the composites C and H, developed by ourselves, its spherical β-phase was determined to be 30% in volume fraction [14]. Apparently, in order to develop the composite S2 containing a desired distinctly increasing volume fraction of the β-phase, the strategy is to shift the compositional point S1 along the line $(Zr_{75}(Ti_{25-x}Nb_x)_{25})_{100-y}$ $(Cu + Ni + Be)_y$ toward the Zr-(Ti + Nb) margin, instead of manipulation of processing method. On the other hand, one should

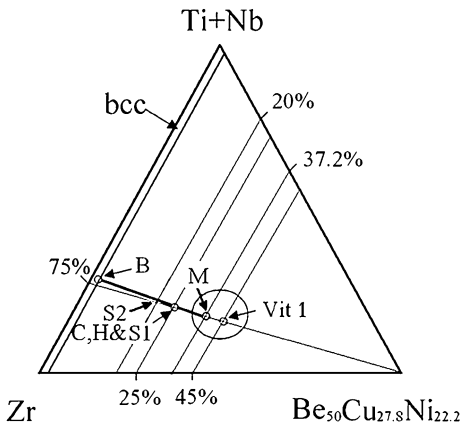

Fig. 1 Pseudo-ternary phase diagram with apexes of Zr, (Ti + Nb), and (Be_{50} + $Cu_{27.8}$ + $Ni_{22.2}$) [17]. S1 and S2 represent the compositional points of composite S1 developed by ourselves and the present composite S2

note that this shift should not be too much. Otherwise, the material would mostly comprise soft β-phase. This would result in a large decrease in strength of the composite material [18]. Therefore, we selected point S2 shown in Fig. 1 as the compositional point of the composite S2, that is, setting $x = 6.66$ and $y = 20$, in the line $(Zr_{75}(Ti_{25-x}Nb_x)_{25})_{100-y}$ $(Cu + Ni + Be)_y$, Thus, the calculated composition of the present composite S2 is $Zr_{60}Ti_{14.7}Nb_{5.3}Cu_{5.6}Ni_{4.4}Be_{10}$.

Experimental procedures

Multicomponent master alloy ingots with a nominal composition of $Zr_{60}Ti_{14.7}Nb_{5.3}Cu_{5.6}Ni_{4.4}Be_{10}$ (at.%) were prepared by arc-melting with pure metal (99.95%Zr, 99.95%Ti, 99.95%Nb, 99.99%Cu, 99.95%Ni, and 98.5% Be) (wt%) under a Ti-gettered argon atmosphere on a water-cooled copper crucible. In order to ensure the compositional homogeneity of the final ingots, a four step melting procedure was adopted [17]. The master alloy ingots were mechanical broken into small pieces and then encapsulated in a quartz tube with 8 mm inner diameter in a vacuum of 4×10^{-3} Pa. The alloy pieces were induction remelted at a temperature above their melting point and then cooled to 900 °C and held at that temperature for 5–8 min. After the holding time, cylindrical samples with a diameter of 8 mm were fabricated by quenching the alloy melt into iced water.

Structural studies were carried out on the transverse sections of the as-cast samples. The phase present in the samples was analyzed by the a Rigaku D/max 2038 X-ray diffractometer (XRD) with Cu Kα radiation. The microstructure was examined by using a JSM-6700-F field emission scanning electron microscope (SEM) and the

phase compositions were determined by an in situ energy dispersive spectrometer (EDS) equipped into the SEM. The volume fraction of the crystalline phase was estimated by the method of dot counting on SEM images. Compression tests were done on specimens with dimensions of 4 mm × 2 mm × 2 mm by using a SANS CMT 4035 testing machine. Mechanical properties were measured at a strain rate of 1×10^{-4} s^{-1} at room temperature. On compression testing, samples were sandwiched between two WC platens, and two blades were mechanically fixed on the side surface of the WC platens. The strain was determined from the displacement between two blades upon loading, which was measured by an YYJ-4/14-Y strain gauge. The detailed shear-band structures formed in the specimen surfaces were observed by a HITACHI S-570 SEM at 25 kV.

Results and discussion

Figure 2 displays the XRD pattern of the as-cast samples of the composite S2, showing sharp diffraction peaks superimposed on a broad scattering hump characteristic of an amorphous phase. The diffraction peaks at $2\theta = 36.24°$, 52°, 65°, 76.6°, and 88° are, respectively, identified as corresponding to bcc β-Zr solid solution (110), (200), (211), (220), and (310). No other phases are detected from the diffraction pattern. This result reveals that the examined samples consist only of the β phase and glassy matrix. Figure 3 is the as-cast microstructure of the present composite. The SEM micrograph shows coarse β phase uniformly dispersed in the glass matrix. It is noted that these β-Zr solid solutions appear mainly to be short-rod-like, worm-like, and nearly spherical in morphology rather than typical dendrite structure with distinct secondary arms. Their average diameter reaches about 20 μm, being much larger than that of typical dendrites which are generally 2–3 μm. The volume fraction of the β phase was estimated to be about 55%. These results demonstrate that a BMG composite with a new composition of $Zr_{60}Ti_{14.7}Nb_{5.3}Cu_{5.6}Ni_{4.4}Be_{10}$ has been developed, which contains a high volume fraction of coarsen ductile inclusions, indicating our success in both modifying alloy composition and controlling solidification process.

The lattice parameter of the β-Zr solid solution is estimated to be $a = 0.3503$ nm from the strongest (110) peak, which is a little different from the examination of $a = 0.3496$ nm reported in [8] but almost identical to the lattice parameter of $a = 0.3525$ nm found by Das et al. for the β-Zr dendrites in the Zr-Nb-(Cu, Ni, Al) nanocrystalline composite [19]. The difference in lattice parameter is thought to be because of the different solid solution degrees of the solute atoms in the β phase, which was produced by

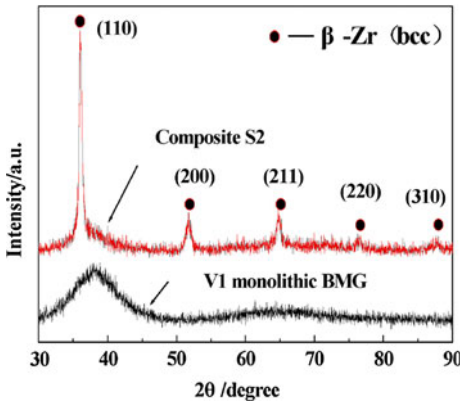

Fig. 2 XRD diffraction pattern for Vit.1 monolithic BMG and as-cast sample of the composite 2

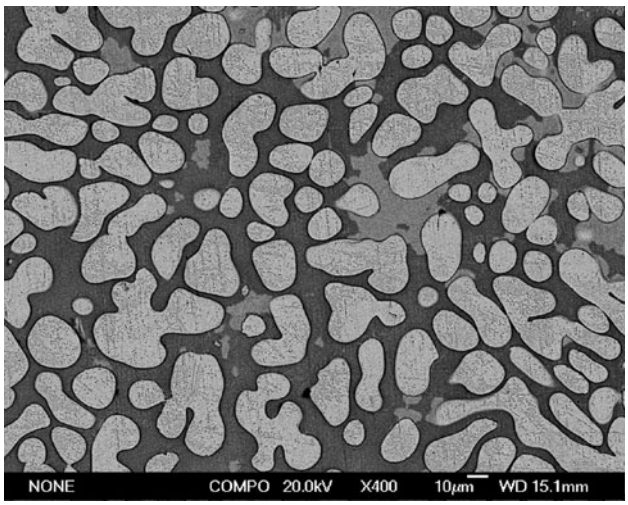

Fig. 3 As-cast microstructure of the composite S2, showing coarse β phase uniformly dispersed in glassy matrix. These β phase inclusions appear to be nearly spherical and worm-like in morphology rather than typical dendrite structure

different rapid cooling techniques. For the β phase inclusions, EDS examinations give an average composition of $Zr_{74.5}Ti_{13.5}Nb_{10}Cu_{1.5}Ni_{0.5}$. This means that the β-Zr solid solution consists mainly of Zr, Ti, and Nb.

The compressive engineering stress–strain curves for the composite S2 and Vit.1 monolithic glass are displayed in Fig. 4. The Curve 1 obtained from the Vit.1 alloy specimen showed immediate failure after linear elastic deformation, without distinct yielding behavior. For two composite samples, the Curves 2 and 3 exhibit significant work hardening and large plastic strain up to 20.36%, causing high fracture strength up to 1,872 MPa. A good combination of the high fracture strength and a large plastic strain demonstrates that the investigated composite possesses excellent mechanical properties at room temperature. Figure 5 is the SEM image of outer shape of the composite specimen No.2 after (Fig. 5a) and before (Fig. 5b)

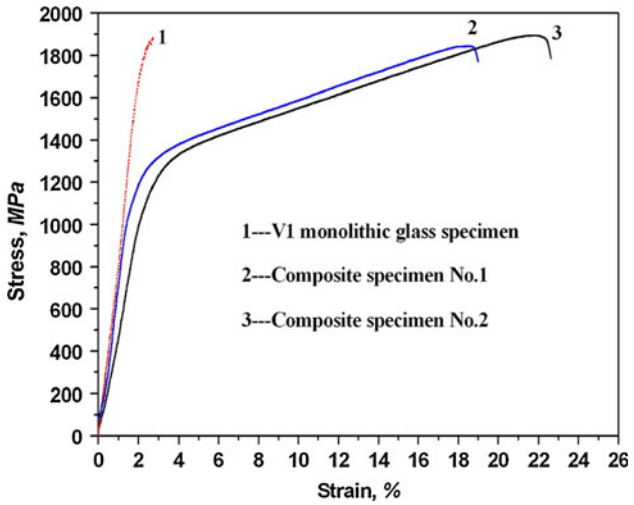

Fig. 4 Engineering stress–strain curves for Vit.1 monolithic glass (*Curve 1*) and Composite S2 (*Curve 2* and *3*) in room-temperature compression tests

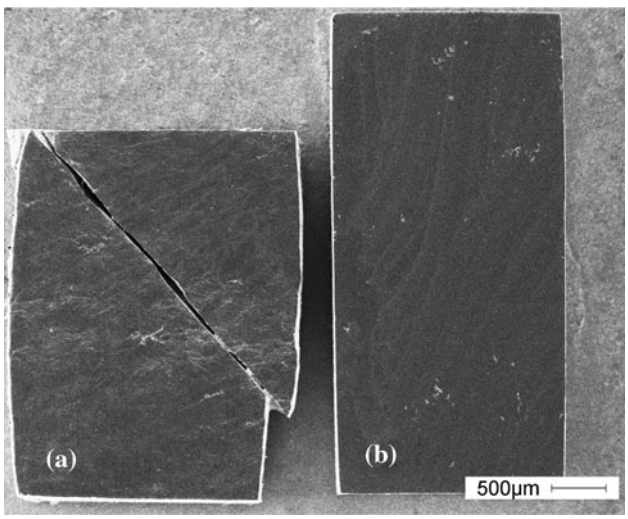

Fig. 5 SEM images of macroscopic appearance of the composite specimen No. 2 after (**a**) and before (**b**) compression test

compression test. It reflects macroscopically observable plastic deformation.

In Fig. 6, the SEM image displays a large number of fine waves uniformly distributed on the outer surface of the fractured specimen. Figure 7 with a higher magnification presents the detailed waves structures. It was found that these waves comprise both the slip bands in the crystalline inclusions and the shear bands in the glassy matrix. This observation suggests that the plastic strain of the present composite originated from two approaches in deformation mechanism. One of them take place to the crystalline β phase through dislocation movement, and the other occurred within the amorphous matrix by the formation of the multi-shear band. Thus, the enhanced plasticity of the composite

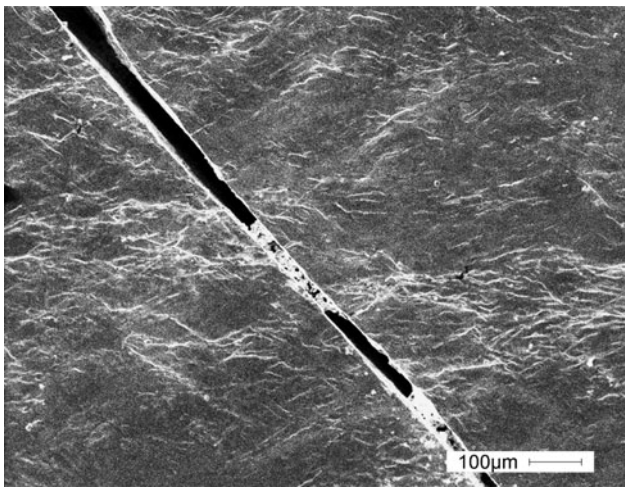

Fig. 6 SEM image of appearance of the composite specimen No. 2 undergoing a large strain of 22.3% to fracture, showing a large number of fine waves uniformly distributed on the outer surface

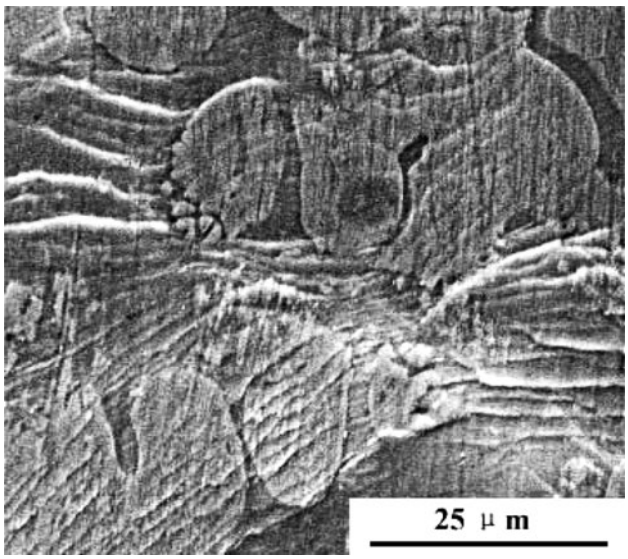

Fig. 7 Magnified image of Fig. 6, displaying details of wave structure

S2 was attributed to the coarsen β phase with a high volume friction. With the increase of the volume friction of the ductile β phase, the deformability of the composite could be improved by plastic deformation originated from dislocation slip within crystalline inclusions. On the other hand, the coarsen β phase is more effective than fine dendrites in hindering shear-band propagation and promoting the formation of multiple shear bands [15, 20].

Conclusions

The microstructures and mechanical properties of BMG composites can be effectively tailored by modifying alloy

composition and controlling solidification process. The present Zr-based BMG in situ composite, with a modified composition of $Zr_{60}Ti_{14.67}Nb_{5.33}Cu_{5.56}Ni4_{.44}Be_{10}$ possesses a desired microstructure of coarsen bcc β-Zr(Ti, Nb) solid solution dispersed throughout in the amorphous matrix. Particles of the β phase, with a high volume fraction of about 55% and a large average size up to 20 μm show nearly spherical or worm-like, instead of typical dendritc structure in morphology. The composite displays a good combination of high fracture strength of 1,890 MPa and large strain up to 22.3% under uniaxial compression at room temperature. The coarse ductile phase with a high volume fraction distributed in the BMG matrix is thought to be primarily responsible for the remarkably improved plasticity of the present composites.

Acknowledgements This work was supported by Natural Science Research Projects of The Education Department of Henan Province China (Grant Nos. 2008A430010 and 2009B430007) and R & D start-up projects of high-level talents of North China University of Water Resources and Electric Power (Grant No. 200709).

References

1. Liu YH, Wang G, Wang RJ, Zhao DQ, Pan MX, Wang WH (2007) Science 315:1385
2. Schroers J, Johnson WL (2004) Phys Rev Lett 93:255506
3. Hofmann DC, Suh JY, Wiest A, Gang D, Lind ML, Demetriou MD, Johnson WL (2008) Nature 451:1085
4. Guo H, Yan PF, Wang YB, Tan J, Zhang ZF, Sui ML, Ma E (2007) Nat Mater 6:735
5. Yim HC, Johnson WL (1997) Appl Phys Lett 71:3808
6. Hays CC, Kim CP, Johnson WL (2000) Phys Rev Lett 84:2901
7. Fan C, Inoue A (2000) Appl Phys Lett 77:46
8. Kuhn U, Eckert J, Mattern N, Schultz L (2002) Appl Phys Lett 80:2478
9. Ma H, Xu J, Ma E (2003) Appl Phys Lett 83:2793
10. Qiao JW, Wang S, Zhang Y, Liaw PK, Chen GL (2009) Appl Phys Lett 94:151905
11. Chen G, Bei H, Cao Y, Gali A, Liu CT, George EP (2009) Appl Phys Lett 95:081908
12. Eckert J, Kuhn U, Mattern N, He G, Gebert A (2002) Intermetallics 10:1183
13. Lee SY, Kim CP, Almer JD, Lienert U, Ustundag E, Johnson WL (2007) J Mater Res 22:538
14. Sun GY, Chen G, Liu CT, Chen GL (2006) Scr Mater 55:375
15. Sun GY, Chen G, Chen GL (2007) Intermetallics 15:632
16. Eckert J, He G, Das J, Löser W (2003) Mater Trans 44:1999
17. Szuecs F, Kim CP, Johnson WL (2001) Acta Mater 49:1507
18. Kim CP (2001) Doctoral degree dissertation, California Institute of Technology
19. Das J, Löser W, Roy SK, Schultz L (2003) Appl Phys Lett 82: 4690
20. Sun GY, Chen G, Chen GL (2007) Mater Sci Forum 539–543:1943